EE

GSI

GSI-95-02
REPORT
FEBRUAR 1995
ISSN 0171-4546

ACCELERATION OF Ta^{10+} IONS PRODUCED BY LASER ION SOURCE IN RFQ "MAXILAC"

V. DUBENKOV, B. SHARKOV, A. GOLUBEV, A. SHUMSHUROV,
O. SHAMAEV, I. ROUDSKOY, A. STRELTSOV, Y. SATOV,
K. MAKAROV, Y. SMAKOVSKY, D. HOFFMANN, W. LAUX,
R.W. MÜLLER, P. SPÄDTKE, C. STÖCKL, B. WOLF,
J. JACOBY

SW gs13

Gesellschaft für Schwerionenforschung mbH
Postfach 110552 · D-64220 Darmstadt · Germany

Acceleration of Ta^{10+} ions produced by laser ion source in RFQ "MAXILAC"

V. Dubenkov, B. Sharkov, A. Golubev, A. Shumshurov,
O. Shamaev, I. Roudskoy
ITEP, Moscow

A. Streltsov, Y. Satov, K. Makarov, Y. Smakovsky
TRINITY, Troitsk

D. Hoffmann, W. Laux, R.W. Müller, P. Spädtke,
C. Stöckl, B. Wolf, J. Jacoby
GSI, Darmstadt

1 Introduction

High current metal ion beams are required for several applications, for example: injection into synchrotrons, material modification or deposition of energy at high density in matter. Various ion sources have been designed and investigated for the production of high current beams [1]. At GSI the CHORDIS [2], [3], MEVVA [4], [5], [6] and Puma (pulsed magnetic field) ECR [7] versions are used for high current beams.

Another possible candidate is the laser plasma ion source, which already has been used on the accelerators in JINR [8] and ITEP [9]. A general description of laser ion sources is given in [10]. In the works carried out in ITEP [11] and CERN [12], it was demonstrated that in carbon dioxide laser plasmas high charge state heavy ions are produced in sufficient numbers to be useful for the complex of accelerators, especially in context with an intensity upgrade of UNILAC.

It has been shown that the beam pulse duration, typically $5 \div 10\mu s$ for a given ion charge state, is due to the range of velocities developed during the expansion of the plasma. Given the number of ions and these pulse lengths , one can produce beam currents up to several hundred of milliamps , after the electrons are separated from the ions in the extraction region. Currents as large as these are difficult to control because of transverse space charge defocussing.

Initial measurements of transverse beam emittance were also done at GSI and CERN:

$$\varepsilon = \frac{1}{\pi} \int dr\, dr' = 100 \text{ mm} \cdot \text{mrad}$$

for an extraction voltage of 40 kV has been obtained.

These integral measurement were made over all ions respectively charge states and time . Therefore it is an upper limit of the emittance for ions of a given charge state.

First experiments at GSI with such a source have been carried out in 1991/1992 [13], [14]. They are described in the first part of this report. The aim of the experiments at that time at the high current test bench at GSI was to get high beam currents and to investigate aspects of beam formation and beam transport with the laser ion source.

As a result of these experiments it was demonstrated that the laser ion source with a 10J CO_2-laser can produce heavy ions in the mA range. The charge states from 5^+ to 10^+ are acceptable for injection into the MAXILAC RFQ structure or into the Wideröe of the UNILAC facility, which requires Z/A = 1/20.

But it was still necessary to show that these ion beams with their measured energy spread ($\Delta E/E \leq 10\%$), current levels and emittances can be formed into beams that can be handled in the beam lines of real accelerator machines.

The aim of the work presented now was to demonstrate the matching of the laser ion source to the GSI RFQ - MAXILAC and to accelerate a beam of mA current of Ta^{10+} ions up to the energy 45 keV/u.

Before the experiments at GSI started, important set of preparations and improvements have been done at ITEP and TRINITY:

1. The laser facility itself and the focusing system in particularly were improved and tested. The tests showed that the laser power density had to be improved by at least a factor of 3.

2. The gas mixture of the laser was experimentally optimized for a maximum production of high charge states heavy ions: Ta^{7+} to Ta^{11+}.

3. A target changing mechanism was developed and installed in the vacuum chamber, giving the possibility to change the target position after a few laser shots, wich has been shown to be necessary.

2 Numerical simulations

Calculations of the parameters of the laser facility has been done to obtain a maximum current of Ta^{10+} ions from the laser produced plasma. For this purpose a quasi 2-D hydrodynamical model of the laser-plasma interaction was developed. In this model self-consistent calculations of multi component plasma expansion, laser energy absorption and ion charge states distribution were carried out. The model was realized in the numerical code "FLY" where the following set of 1-fluid 2-temperature hydrodynamic equations combined with the set of ionisation-recombination equations were solved using a Lagrangian difference scheme:

$$\frac{\partial n_1}{\partial t} = -\frac{n_1}{V}\frac{\partial V}{\partial t} \tag{1}$$

$$\rho\frac{\partial u_x}{\partial t} = -\frac{\partial}{\partial x}(p_e + p_i) \tag{2}$$

$$\rho\frac{\partial u_r}{\partial t} = -\frac{2}{r}(p_e + p_i) \tag{3}$$

$$\frac{3}{2}\frac{\partial T_e}{\partial t} + p_e\frac{\partial}{\partial x}\left(\frac{1}{n_e}\right) = \frac{1}{n_e}\left(Q_{las} - Q_{ei} - Q_{ri} - \frac{\partial q_e}{\partial x}\right) \tag{4}$$

$$\frac{3}{2}\frac{\partial T_i}{\partial t} + p_i\frac{\partial}{\partial x}\left(\frac{1}{n_i}\right) = \left(\frac{1}{n_i}\right)Q_{ei} \tag{5}$$

$$\frac{dN_z}{dt} = N_{z-1}\mathcal{K}_{z-1} - N_z\mathcal{R}_z - N_z\mathcal{K}_z + N_{z+1}\mathcal{R}_{z+1} \tag{6}$$

Here T_e, T_i - electron and ion temperature in eV; n_e, n_i - electron and ion concentations in cm^{-3}; p_e, p_i - electron and ion pressure; ρ - plasma density; u_x, u_r

– normal and radial plasma velocity components (axis X is perpendicular to the taget surface); N_z – the number of ions in a Z charge state in a spesific volume $v = 1/n_i$; $\mathcal{K}_z$, $\mathcal{R}_z$ – the total ionization and recombination rates of Z charged ions. The radiative, dielectronic and three body recombination as well as the electron impact ionization were taken into account.

The electron-ion temperature relaxation is described by the term Q_{ei}:

$$Q_{ei} = \frac{3m_e}{m_i} n_e \nu_{ei} (T_e - T_i),$$

where m_e, m_i – electron and ion masses; ν_{ei} is the frequency of electron-ion collisions:

$$\nu_{ei} \simeq 3 \cdot 10^{-6} \frac{n_i Z^2 \Lambda_{ei}}{T^{3/2}} \qquad [c^{-1}].$$

Here Λ_{ei} is the Coulomb logarithm for electron-ion collisions.

The term Q_{ri} describes the internal energy changing due to ionization and recombination processes:

$$Q_{ri} = n_e n_i \sum_z \Big(\mathcal{K}_z^i (\tfrac{3}{2} T_e + I_z) - \mathcal{R}_z^t (\tfrac{3}{2} T_e + \mathcal{E}) \Big).$$

Here $\mathcal{K}_z^i$ – electron impact ionization rate, $\mathcal{R}_z^t$ – three body recombination through high exited levels, I_z – ionization potential of Z-charged ions, and $\mathcal{E}$ is described by the equation:

$$\mathcal{E} \simeq 1.4 \cdot 10^{-10} \frac{(n_e/Z)^{2/3}}{T_e} \qquad [eV].$$

The term q_e in the equation (4) is an electron heat conduction flux:

$$q_e = \min \begin{cases} \kappa \nabla_x T_e \\ \sqrt{2/\pi}\, n_e T_e \sqrt{T_e/m_e} \end{cases},$$

where κ is an electron heat conductivity coefficient:

$$\kappa \simeq 10^{22} \frac{T_e^{5/2}}{(Z+4)\Lambda_{ei}} \qquad [cm^{-1}c^{-1}]$$

The laser energy absorbtion is described by the term Q_{las}:

$$Q_{las} = k(x)q_{las}\Big(\exp\Big(-\int\limits_{-\infty}^{x} k(x)\,dx\Big)+\exp\Big(-\int\limits_{-\infty}^{x_c} k(x)\,dx-\int\limits_{x_c}^{x} k(x)\,dx\Big)\Big).$$

Here q_{las} is the incident laser radiation flux and $k(x)$ is the inverse bremstrahlung absorption coefficient:

$$k(x) = \frac{4\sqrt{2\pi}\,Z^2e^4n_i\Lambda_{ei}}{3cT_e^{3/2}m_e^{1/2}}\frac{\left(\frac{n_e(x)}{n_c}\right)^2}{\left(1-\frac{n_e(x)}{n_c}\right)^{1/2}}.$$

Here c – vacuum speed of light; n_c, x_c – critical density and position of the critical surface.

The code "FLY" was tested in a rather wide set of laser irradiation power densities - from 10^9 to 10^{14} W/cm$_2$ for wave length from 0.69 to 10.6 μm. A good agreement with experimental data was found in the main plasma parameters - plasma temperature in the heating stage, ion energies and ion charge states.

According to the obtained results, the maximum ion current of Ta^{10+} at a distance 70 cm away from the target can be reached using a laser pulse with a power density of about $4{\cdot}10^{11}$ W/cm^2 and half width pulse duration of about 50 ns. The spot size is a function of the available laser energy. The increase of spot size leads to an increase of the ion current. In particular for the case of the laser pulse energy of 1J the total ion current density should reach 10mA/cm^2 at the distance 70 cm away from the target.

3 Experimental setup

The experimental setup consists of six main parts: laser, optical system, source chamber, matching system, RFQ-accelerator and beam diagnostics (see Fig. 1).

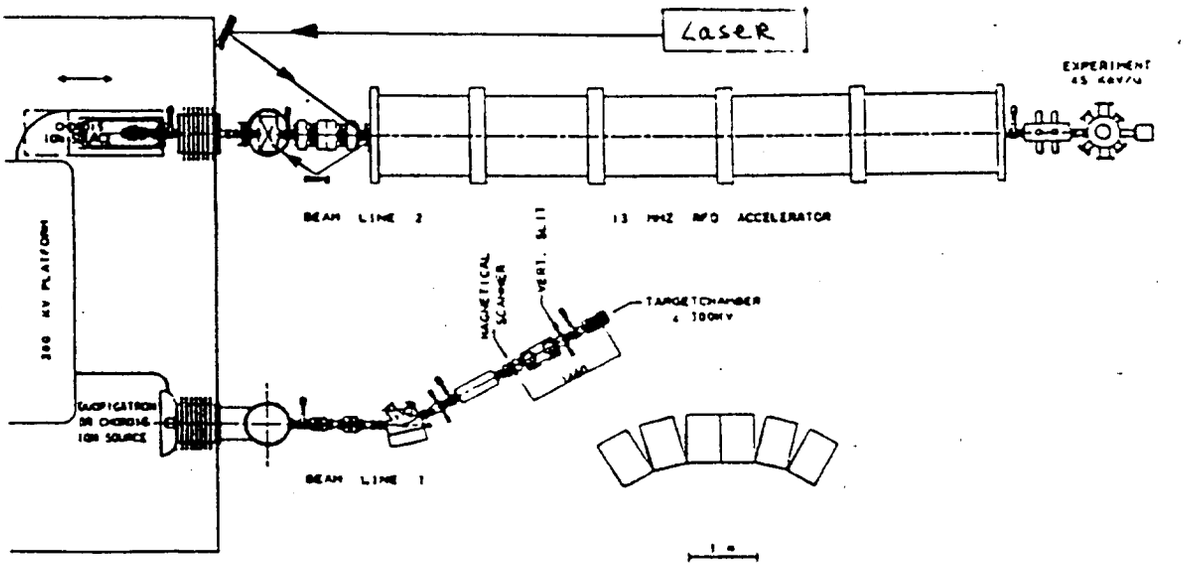

Fig. 1: Experimental setup.

3.1 Laser

A CO_2 laser is used to evaporate particles from a target which is made out of the material to be ionized. The pulse energy of the laser is about 4J in a pulse of 1 μs on the ground, with a repetition rate of up to 1Hz. However, the first peak of the laser power responsible for the plasma heating is about 50 ns (half width) and contains about 25% of pulse energy (see Fig. 2).

The unstable resonator consisting of two confocal mirrors ($F_1/F_2 = 1/3$) provides the divergence of the laser beam of $\simeq 0.3$ mrad.

The laser pulse shape influences the charge state distribution in the generated plasma, and depends critically on the ratio of the three gases in the mixture. The ratio of CO_2 :N_2 :He was experimentally determined with 4:1:7 to be favorable for higher charge state production.

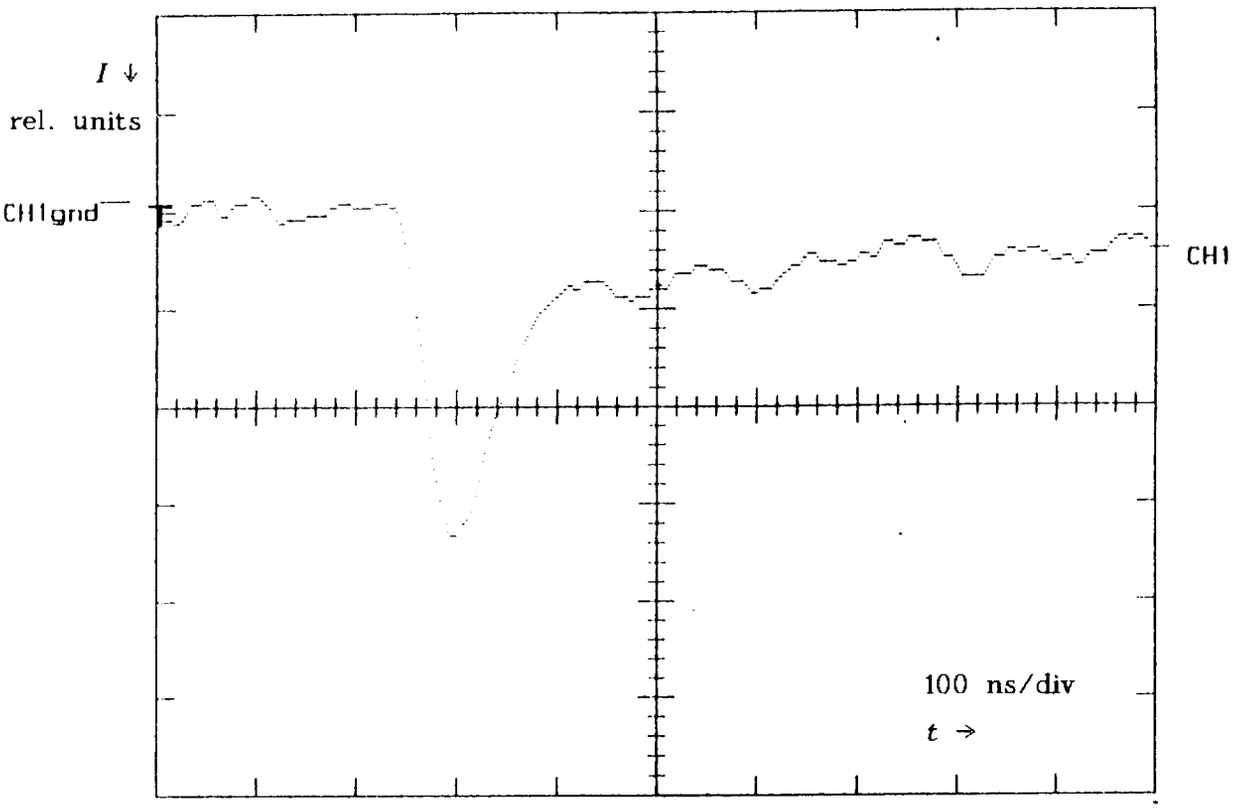

Fig. 2: Laser pulse shape.

3.2 Source chamber and optical system

The cylindrical source chamber has a diameter of 350 mm and is 300 mm high. Beside the optical system it contains only the target mounted on a target changing mechanism. The changing of the target position after a few shots is necessary due to the destruction of the target by laser. The distance between the target and the extraction system is 690 mm. This distance was chosen experimentally to get the necessary particle density in front of the extraction system as well as to provide the wanted ion pulse duration, which is due to the range of velocities developed during the expansion of the plasma.

The laser beam enters the target chamber, which is at a potential of $\simeq$50 kV, through a NaCl window. The source chamber is pumped down to $2 \div 3 \cdot 10^{-6}$ torr.

The optical system consists of four flat copper mirrors (see Fig. 1) directing the laser light on the fifth one — a spherical reflector F=172 mm which focuses the laser light on the surface of the solid target. The focus spot size is about 70μm, corresponding to a power density of $\simeq 5 \cdot 10^{11}$ W/cm^2 .

The resulting plasma expands hydrodynamically into the vacuum, and a part of it is extracted by the extraction system.

3.3 Matching system

The matching section was developed to get the beam parameters according to the injection requirements of the RFQ structure — injection energy, radius and convergence angle of the beam. It consists of the extraction system integrated with an

einzel lens (Fig. 3) and two grids. The extraction system has two electrodes with a hole of 22 mm and a 16 mm gap.

The shapes of the electrodes profile of the einzellens, electrodes and the potential distribution of the whole system were designed and manufactured according to the results of numerical simulation by using the "AXCEL" code [15]. Fig. 3 shows the results of a typical run for j=6.5 mA/cm^2 Ta^{9+} beam.

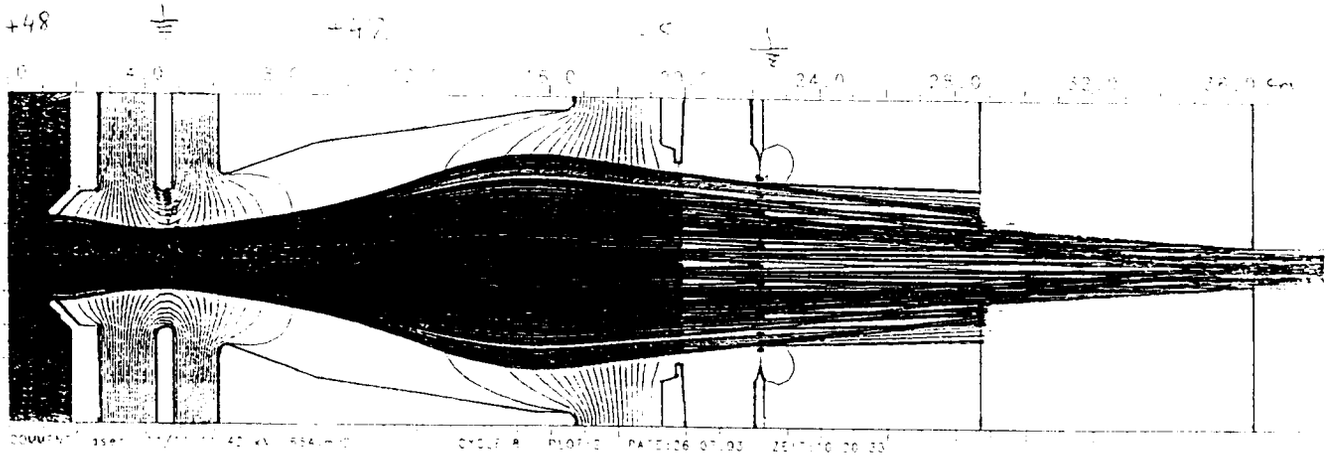

Fig. 3: "AXCEL"-simulation, showing the matching section.

The negative grid seems to give a considerable positive effect preventing the reverse motion of electrons captured by a potential well of the intense beam. Because of the good vacuum ($\simeq 10^{-4}$ Pa) the secondary electrons are created most probably with collisions of the primary beam at apertures.

The correct potential distribution given in fig. 3 provides a good focusing of the extracted beam in the acceptance cone of the RFQ accelerator. One can conclude a good correlation of the theory and experiments.

3.4 RFQ-accelerator

The GSI RFQ "MAXILAC", 13.37 MHz, with an aperture of$\simeq$ 12 mm, was used for the experiments. The injection energy is 2.4 keV/u, the output energy 45 keV/u. The accelerator consists of five sections containing 168 $\beta\lambda/2$ cells. An empirical formula gives the upper limit for the possible accelerated current due to space charge effect: $I_{max} \simeq 0.1$ A/q (A/q — mass to charge ratio). For Ta^{10+} this relation gives 1.8 mA.

4 Measurements

4.1 Current measurements

The current measurements of the accelerated Ta ion beam have been carried out by means of a Faraday cup placed $\approx$ 100 cm behind the exit flange of the RFQ. A typical integrated current signal (1 μs integration time) is shown in Fig. 4.

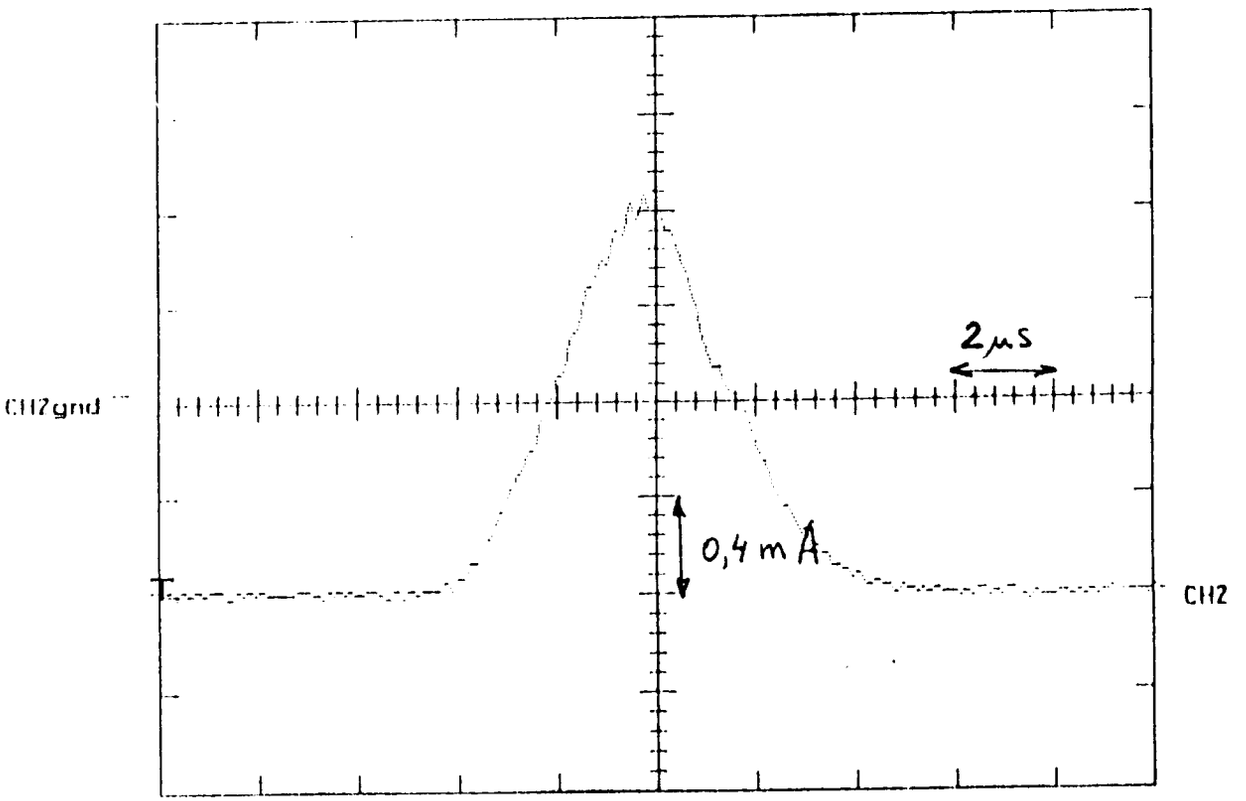

Fig. 4: Integrated Current vs time.

The average value of accelerated current is about 1.8 mA in a 4 μ s pulse of Ta^{10+} ions. The best results were obtained by applying 40 kV to the extraction electrode and 35 kV on the einzellens. The potential of the negative grid was $\simeq$-2 kV. The accelerated current is close to the upper limit of the RFQ structure. The fine structure of the accelerated beam signal represents the sequence of 10 ns bunches

with a 75 ns period (13.37 MHz). The bunch amplitudes are up to 9 mA (Fig. 5).

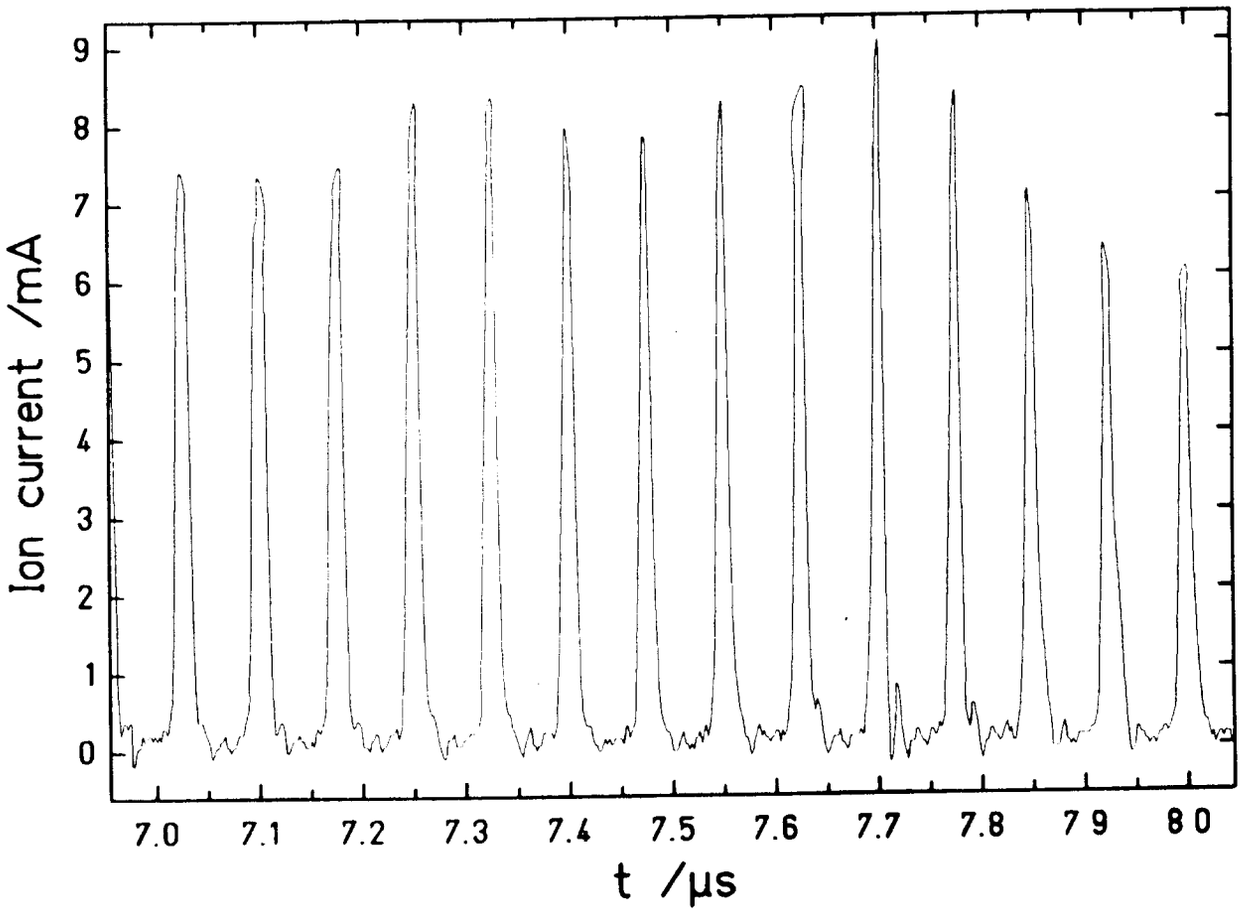

Fig. 5: Bunch structure of the Maxilac Ta beam.

4.2 Charge analysis of accelerated beam

Simple calculations show that the accelerated pulse could contain the mixture of Ta^{10+} and Ta^{11+} ion charge states simultaneously. To check the content of Ta^{11+} in the Ta^{10+} 45 keV/u beam, an electrostatic deflection system was installed 156 cm behind the RFQ exit aperture. The image of the beam behind the deflector was detected by a scintillator screen placed 62 cm behind. The electrostatic deflector has two 15 cm long parallel plates with 28 mm gap. Without any applied voltage the beam produces a bright spot on the scintiliator screen, like that shown in Fig. 6 a. By applying 12.5 kV to the deflector electrodes the spot splits in two parts which

correspond to Ta^{10+} and Ta^{11+} (Fig. 6 b).

Fig. 6: Beam Image without deflection (a) and with deflection (b).

The identification of the charge states follows simple TOF relations and the equation of motion in a homogeneous electric field. A PCO camera has been used for registration of the light emission signal from the screen.

The intensity difference of the split parts in Fig. 7b shows that the accelerated beam contains about $\approx 70\% Ta^{10+}$ and $\approx 30\% Ta^{11+}$ ions.

For time resolution a streak camera was used instead of the PCO . The time delay $\Delta t \approx 0.6\mu$s between Ta^{11+} and Ta^{10+} could be explained taking into account a slight difference in the velocity spectra of highly charged ions in laser produced plasma, when the plasma expands from the target to the extraction region, and due to the velocity dependence on charge after the extraction. (The RFQ system tolerates the energy spread of injected ions $\Delta E/E \approx 10\%$).

4.3 Injected current

For the measurement of total ion beam current injected into the RFQ a Faraday cup was placed just behind the matching section. According to the velocity spectra obtained in Troitsk at similar conditions, the first part of the signal from 6 to 16 μs represents the mixture of the higher ion charge states from 8^+ to 11^+.

The current amplitude is more than 10 mA . Since the exact charge state distribution was not measured one can roughly presume the injected current of Ta^{10+} ions to be between 2 and 5 mA. The comparison of these data with real accelerated current obtained ($\approx$ 1.8 mA) gives reason to conclude the transmission of the RFQ to be from 50% to 20%.

References

[1] The Physics and Technology of Ion Sources ed. I. G. Brown.

[2] R. Keller, Proc. Lin. Acc. Conf, Stanford 1986, SLAC-303, p. 232, Stanford, CA, 1986.

[3] R. Keller et al. Vacuum 36, 833, 1986.

[4] P. Spädtke et al. Report GSI-88-20, GSI, Darmstadt, 1988.

[5] B.H. Wolf et al. Rev. Sci. Instr., 61 II, 408, 1990.

[6] B.H. Wolf, Proc. Int. Symp. on Discharges and Electrical Insulation in Vacuum, Darmstadt 1992, VDE-Verlag Berlin, Offenbach 1992.

[7] U. Ratzinger, Überlegungen zur Entwicklung einer gepulsten ECR-Quelle und zu ihren Einsatzmoglichkeiten in Synchrotron-Injectoren, GSI-UNILAC-INT/89-3, 1989.

[8] Yu.D. Beznogich et al, Preprint JINR, Dubna, P9-84-251, 1984.

[9] L.S. Barabash et al, Laser and Particle Beams, 1984, v.2, p. 49-59.

[10] R. H. Hughes and R.J. Anderson, Laser Ion Sources, in: "The Physics and Technology of Ion Sources", ed. I.G. Brown.

[11] B. Sharkov et al, Rev. Sci. Instr., V. 63, p. 2841, 1992.

[12] Y. Amdiduche et al, Rev. Sci. Instr. V. 63, p. 2838, 1992.

[13] G. Beljaev et al, Laser Plasma Ion Sources for Intense Heavy Ion Beams, GSI Report, GSI-91-2, 1991.

[14] V. Dubenkov et al., A Laser Source for High Current High Charge State Ion Beam, GSI Report, GSI-93-1, 1993.

[15] P. Spädtke, AXCEL-GSI, GSI report 83-9, 1983.